Annals of Nuclear Medicine Vol. 11, No. 2, 55–66, 1997

Recent advances in nuclear cardiology in the study of coronary artery disease

Nagara TAMAKI,* Eiji TADAMURA,** Takashi KUDOH,**
Naoya HATTORI,** Masayuki INUBUSHI** and Junji KONISHI**

*Department of Nuclear Medicine, Hokkaido University School of Medicine
**Department of Nuclear Medicine, Kyoto University Faculty of Medicine

A variety of new radiopharmaceutical agents have been introduced to probe myocardial function *in vivo*. This review will introduce these new techniques which have recently been available in Japan. Tc-99m perfusion imaging agents provide excellent myocardial perfusion images which may enhance diagnostic accuracy in the study of coronary artery disease. In addition, greater photon flux from the tracer permits simultaneous assessment of regional perfusion and function with use of first-pass angiography or ECG-gated acquisition. Positron emission tomography enables metabolic assessment *in vivo*. Preserved FDG uptake indicates ischemic but viable myocardium which is likely to improve regional dysfunction after revascularization. In addition, FDG-PET seems to be valuable for selecting a high risk subgroup. Recently I-123 BMIPP, a branched fatty acid analog, has been clinically available in Japan. Less uptake of BMIPP than thallium is often observed in the ischemic myocardium. Such perfusion metabolic mismatch which seems to be similarly observed in FDG-PET is identified in the stunned or hibernating myocardium with regional dysfunction. Both of them are likely to recover afterwards. Severe ischemia is identified as reduced BMIPP uptake at rest, suggesting its role as an ischemic memory imaging. I-123 MIBG uptake in the myocardium reflects adrenergic neuronal function *in vivo*. In the study of coronary artery disease, neuronal denervation is often observed around the infarcted myocardium and post ischemic region as well. More importantly, reduced MIBG uptake in these patients can identify high risk for ventricular arrhythmias and assess severity of congestive heart failure. These new techniques will provide insights into new pathological states in the ischemic heart disease and enable to select optimal treatment in these patients.

Key words: emission computed tomography, ischemic heart disease, myocardial perfusion, BMIPP, MIBG

INTRODUCTION

ISCHEMIC HEART DISEASE is quite common caused by reduced coronary artery blood flow to the myocardium and is the most frequent cause of death in the USA and second cause of death in Japan as well. Coronary angiography has been widely used for final diagnosis and management of patients with coronary artery disease. However, radionuclide studies can noninvasively demonstrate regional myocardial perfusion at rest and during stress and this may provide important information for the accurate diagnosis and management of patients with coronary artery disease.

Recently, a variety of radiopharmaceutical agents have been introduced to probe myocardial function *in vivo*. These new techniques will provide new insights into myocardial pathophysiology in ischemic heart disease. This review will introduce the new techniques which have recently become available in Japan.

Based on an invited educational lecture at the 6th Asia and Oceania Congress of Nuclear Medicine and Biology, and the 36th Annual Meeting of the Japanese Society of Nuclear Medicine, Kyoto, October 1996.

For reprint contact: Nagara Tamaki, M.D., Department of Nuclear Medicine, Hokkaido University School of Medicine, Kita-15, Nishi-7, Kita-ku, Sapporo 060, JAPAN.

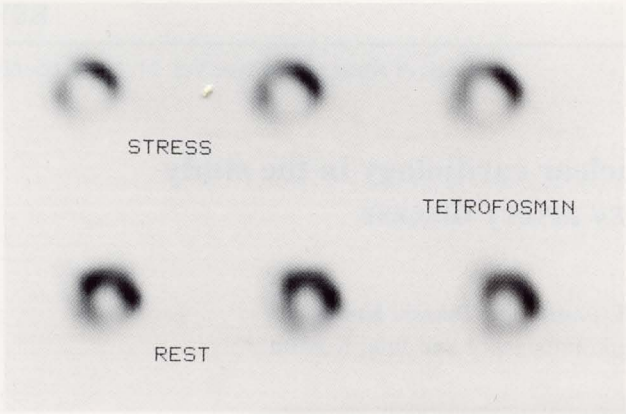

A

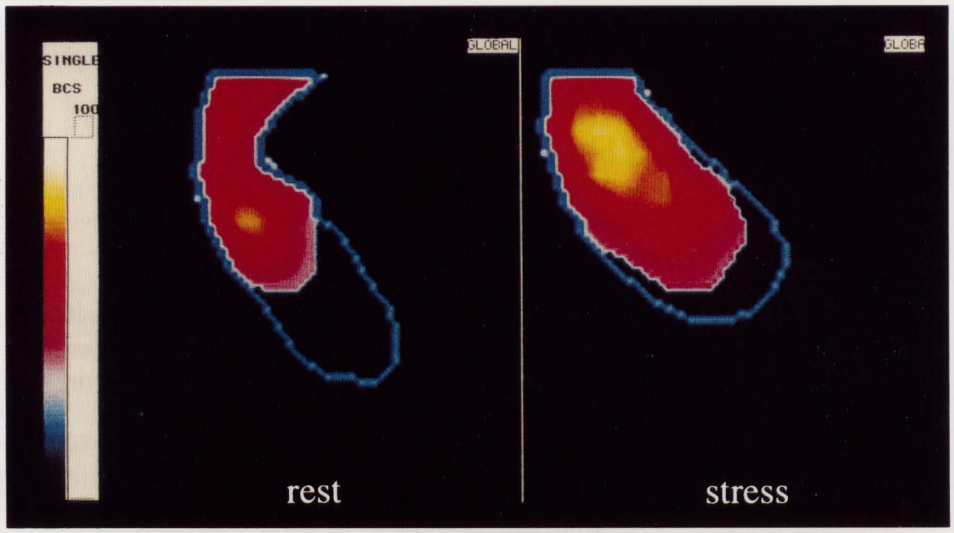

B

Fig. 1 A series of short-axis slices of myocardial perfusion images at stress and rest using Tc-99m tetrofosmin (A) and radionuclide ventriculograms (B) both at rest (left) and stress (right) at the time of tracer administrations in a patient with severe coronary artery disease.

I. Evaluation of myocardial perfusion

Evaluation of myocardial perfusion during exercise is of clinical importance for the diagnosis of ischemic heart disease. Thallium-201 chloride has been widely used for the detection and viability assessment of coronary artery disease.[1–3] However, the long physical half life of the tracer and the low-energy photons emitted from thallium-201 may limit its value as a tracer for myocardial perfusion analysis.

To minimize these physical limitations of thallium-201, a group of technetium-99m labeled compounds have been developed. Among them, Tc-99m methoxy isobutyl isonitrile (sestamibi) provided the best biologic properties for clinical applications.[4–9] However, it requires heating for the preparation of the tracer and it is necessary to wait for 40–60 minutes before imaging after injection due to the clearance of liver activity.

Recently, Tc-99m-1,2-[bis(2-ethoxyethyl)phosphino] ethane (tetrofosmin) has been introduced. This compound showed favorable characteristics, including high myocardial uptake and retention, and more rapid clearance from the liver. In addition, this agent can be labeled with Tc-99m at room temperature and without heating.[10–14] The phase I clinical study confirmed the safety of this radiopharmaceutical and provided excellent myocardial images with rapid clearance from the blood.[11]

These Tc-99m labeled perfusion agents have provided excellent myocardial images which provided better diagnostic accuracy for the detection of coronary artery disease with lower false positive rate than thallium-201. In addition, greater photon flux obtained with these agents permits first-pass study at the time of administration[15–20] or ECG-gated acquisition for the imaging.[21–24] These techniques permit simultaneous analysis of regional myocardial perfusion and function, which is of clinical importance for the evaluation of coronary artery disease.

Figure 1 shows a series of short-axis slices of myocardial perfusion images at stress and rest obtained with Tc-99m tetrofosmin and radionuclide ventriculograms both at rest and during stress in a patient with severe coronary artery disease. A medium-sized perfusion defect is seen in the inferior region at rest with stress-induced ischemia is noted in anterior and septal region on these perfusion images. The regional wall motion is normal with LVEF of 51% at rest. However, severe regional asynergy is seen with reduction in LVEF to 38% during stress, indicating poor ventricular function during stress despite normal function at rest. Such combined assessment of perfusion and function at the time of tracer administration can be obtained. This technique provides clinically important indices for the assessment of severity of myocardial

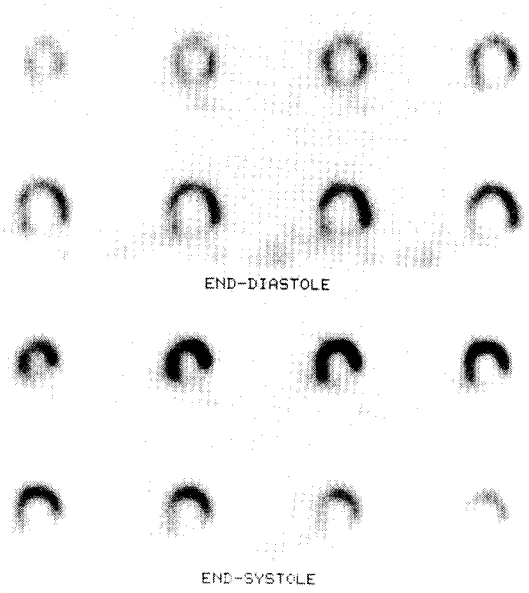

Fig. 2 A series of short-axis slices at end-diastolic (top) and end-systolic (bottom) phases in a patient with inferior wall myocardial infarction obtained by ECG-gated SPECT images 60 minutes after Tc-99m sestamibi administration at rest.

ischemia and prognosis in these patients.

Figure 2 shows a series of short-axis slices in end-diastolic and end-systolic phases in a patient with inferior wall myocardial infarction which was obtained by ECG-gated SPECT images 60 minutes after Tc-99m sestamibi administration at rest. A large perfusion defect is observed in the inferoposterior region in the end-diastolic and end-systolic phases. However, regional wall thickening is well demonstrated in the remaining myocardium despite no regional wall thickening in the inferior region, indicating normal ventricular function at rest. This type of analysis permits assessment of regional function such as wall thickening and global function as well such as volume and ejection fraction calculation. Recently, change in wall thickening caused by low-dose dobutamine is also quantitatively measured by gated myocardial perfusion SPECT in order to assess inotropic functional reserve, and thus, tissue viability.[25]

The prognosis for patients with coronary artery disease is related to the degree of impairment of resting and exercise ventricular function[26,27] and the severity of reversible perfusion abnormality.[28,29] The combined assessment of regional perfusion and function should therefore, have a prognostic value as well as a diagnostic value in the evaluation of these patients.[30,31]

Our preliminary comparative study of regional perfusion and wall motion at stress in the segments showed concordant score in 42–50% of them.[20] On the other hand, the remaining 50% of segments showed discordant findings for stress perfusion and wall motion. Interestingly, many segments showed greater severity in wall motion abnormality than in regional perfusion at rest, but a smaller number of segments showed similar findings at stress. This may be partly due to stunned myocardium where perfusion recovered but ventricular dysfunction persisted.[32] These data indicate that regional wall motion and perfusion may provide rather independent parameters of regional function. Thus, the first-pass radionuclide ventriculography may provide important and valuable information in the regional myocardial condition, which seems to be rather independent of regional perfusion.

Another important aspect of Tc-99m perfusion agent is to freeze myocardial perfusion at the time of tracer administration. This advantage permits evaluation of the area at risk in patients with acute myocardial infarction on admission. When the tracer is administered on admission, the perfusion images obtained after emergency revascularization therapy may reflect myocardial perfusion on admission. When another perfusion study is done several days after revascularization therapy, the location and amount of salvaged myocardium can be accurately analyzed.[33–35]

Some reported that the residual uptake of Tc-99m perfusion tracer may reflect tissue viability.[36–39] Udelson et al.[39] reported that the Tc-99m sestamibi uptake correlated well with redistribution thallium activity and can differentiate reversible ischemia from irreversible myocardial scar. It is, however, controversial whether the residual uptake of Tc-99m perfusion tracer may accurately reflect tissue viability, compared to thallium redistribution or positron emission tomography.[40–42]

Because of superior physical characteristics, myocardial perfusion studies with Tc-99m perfusion agents have become more popular recently all over the world. Similarly, these new agents are expected to be more widely used in Japan. However, since the chemical characters of these agents are slightly different from those of thallium, a more careful comparisons may be warranted for deciding the optimum perfusion tracer for a variety of conditions in the assessment of coronary artery disease.

II. Evaluation of myocardial metabolism

The advantage of tracer techniques is to use a radiolabeled compound for *in vivo* quantification of specific biological processes. With introduction of positron emission tomography (PET), the spectrum of *in vivo* tissue characterization has been widened with use of physiological tracers labeled with C-11, N-13, O-15 and F-18 which allow the synthesis of naturally occurring and biologically active compounds. In parallel with advances in imaging technologies, cardiovascular research has extended beyond the evaluation of myocardial perfusion and function in various cardiac diseases. For example, the importance of energy metabolism in maintaining the integrity of cardiac performance has been increasingly recognized with PET.

Table 1 summarizes positron labeled compounds which

Table 1 Positron emitting tracers comonly used in the study of cardiac PET

Category / Compounds	Function (Mechanism)
Tracers of blood flow	
N-13 ammonia	(Metabolic trapping)
Rb-82	(Sodium-potassium pump)
O-15 water	(Diffusion)
Cu-62 PTSM	(Lipophilicity)
C-11 (Ga-68) albumin microsphere	(Capillary blockage)
Tracers of metabolism	
C-11 palmitate	Fatty acid metabolism
F-18 2-fluoro 2-deoxyglucose (FDG)	Exogenous glucose utilization
C-11 acetate	Oxidative metabolism
O-15 oxygen	Oxygen consumption
C-11 (N-13) amino acids	Amino acid metabolism & protein synthesis
Tracers of innervations	
F-18 metaraminol	Adrenergic neuron density
C-11 hydroxyephedrine	Adrenergic neuron density
Tracers of receptors	
C-11 methyl QNB	Muscarinic receptor function
C-11 CGP-12177	Beta-adrenergic receptor function
C-11 practorol	Beta-adrenergic receptor function
C-11 PK-11195	Benzodiazepine receptor function
Other tracers	
F-18 misonidazole	Hypoxic and ischemic tissue
O-15 (C-11) carbon monoxide	Blood pool

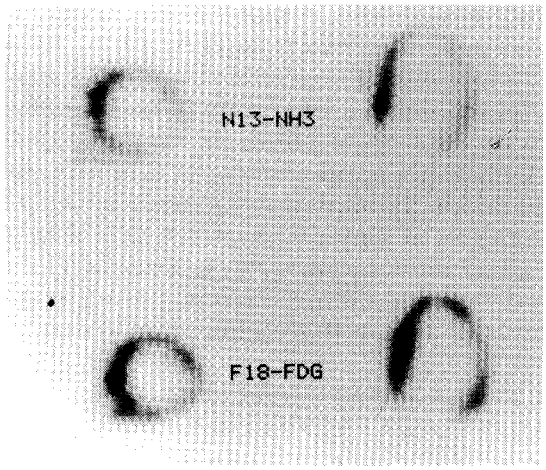

Fig. 3 Representative short-axis (left) and vertical long-axis slices of N-13 ammonia perfusion images (top) and F-18 FDG glucose metabolic images (bottom) of a patient with coronary artery disease. Preserved FDG uptake relative to perfusion (so called perfusion-metabolism mismatch) is observed in inferolateral regions, indicating presence of myocardial ischemia.

are commonly employed in the study of cardiac PET. Among them, N-13 ammonia as a marker of myocardial perfusion and FDG as a marker of exogenous glucose utilization are commonly used in the clinical cardiac PET studies.

FDG, the most important radiopharmaceutical for the clinical application of cardiac PET, is transported across membranes and phosphorylated to FDG-6-phosphate in the myocyte. Because FDG-6-phosphate does not enter glycolysis or participate in glycogen synthesis, the radioactivity in the tissue may represent the integral of glucose phosphorylation. Thus, imaging of tissue FDG uptake permits the assessment of exogenous glucose utilization.[43] The myocardium can use various substrates for its energy metabolism. The major energy source for high energy phosphate (ATP) production is oxidation of long-chain fatty acids. Carbohydrates play a rather minor role in the myocardial substrate metabolism in the fasting state. After carbohydrate exposure, on the other hand, glucose becomes an important source for oxidative metabolism, so that the relative contribution of each substrate to myocardial metabolism depends on the substrate availability in plasma, the hormonal milieu, and the cardiac workload.[44-46]

Early laboratory studies indicated that utilization of exogenous glucose is accelerated in acutely ischemic myocardium and fatty acid oxidation is rapidly reduced.[44-46] These data imply that the use of FDG can be used for identifying ischemic myocardium. In the hypoperfused regions on the N-13 ammonia perfusion studies, accelerated glucose utilization was identified by the relative increase in FDG uptake in the ischemic areas. The areas with such perfusion-metabolism mismatch may represent ischemic myocardium (Fig. 3), and those with concordant decrease in perfusion and glucose metabolism may represent scar tissue.[47]

FDG-PET has been considered as a gold standard for tissue viability in noninvasive clinical studies to predict the recovery of cardiac function after revascularization. A number of reports showed that FDG uptake in the presence of reduced flow was highly predictive for recovery, while the absence of metabolic activity in the segments with perfusion defect was associated with lack of recovery in contractile function.[48–52]

Redistribution thallium imaging has been widely used for identifying ischemic and viable myocardium. Preserved glucose metabolism was observed in the areas with redistribution on stress thallium scan.[53] However, preserved glucose metabolism was also observed in the areas of persistent thallium defect,[54–56] supporting the underestimation of tissue viability on stress-redistribution thallium scan. On the other hand, when FDG findings were compared to the stress-reinjection thallium findings, a closer correlation was expected.[57] However, FDG-PET seems to be slightly more sensitive for detecting ischemic myocardium.[58] These data indicate that identification of residual metabolic activity has advantages over thallium perfusion imaging, since metabolic imaging provides a better quality positive signal in the viable myocardium, and perhaps more accurate information regarding reversibility than the residual perfusion or membrane potential on thallium imaging.

Another clinical importance of FDG-PET is that it may select a high risk subgroup in patients with coronary artery disease. Eitzman et al.[59] and our group[60] both showed a high incidence of cardiac complications in patients with decreased perfusion and enhanced glucose utilization. Our preliminary results in the follow-up study of patients with myocardial infarction showed a slightly higher predictive value for future cardiac events obtained by FDG-PET than that by the routine stress thallium scan. More importantly, the incidence of cardiac events in patients with a perfusion-metabolism mismatch can be reduced by revascularization.[59,61] These results also support that those with reduced perfusion and enhanced glucose metabolism are good candidate for revascularization predicated on the concept of improving regional cardiac function and reducing future cardiac events.

Based on the hypothesis that viable tissue requires oxygen to maintain cell survival, C-11 acetate has been proposed as a marker of tissue viability. Following administration of C-11 acetate, this is activated to acetyl CoA, oxidized in mitochondria by the TCA cycle, and washed out of the myocardium as C-11 CO_2 and H_2O. The early clearance rate in the myocardium measured by serial dynamic PET study corresponds closely to release of C-11 CO_2 from the myocardium, and it may therefore represent oxidative metabolism.[62,63] The major advantage of this tracer is that, unlike glucose metabolism, the clearance rate constant was not influenced by plasma substrate levels.[64]

Gropler et al.[65] showed the preliminary results indicating the areas with preserved oxidative metabolism as reversible ischemic tissue which is likely to improve regional asynergy after revascularization. The predictive value of C-11 acetate PET was slightly better than that of FDG-PET. The experimental study also supports the idea that the functional recovery after reperfusion was associated with the recovery of oxidative metabolism.[66] We have recently reported that oxidative metabolic reserve after low-dose dobutamine infusion was a better marker of the recovery of regional function than resting oxidative metabolism.[67] Such an interventional study may play a more important role in assessing tissue viability.

Long chain fatty acids are the most important energy-yielding substrate for oxidative metabolism in the normal myocardium. Approximately 60–80% of ATP produced in aerobic myocardium derives from fatty acid oxidation. In ischemic myocardium, on the other hand, oxidation of free fatty acids is greatly suppressed and glucose metabolism plays a major role in residual oxidative metabolism.[44,45] In myocardial necrosis, since there will be no further metabolism, preserved glucose metabolism is considered to be an important marker of ischemic but viable myocardium, while alteration of fatty acid oxidation is considered to be a sensitive marker of ischemia or myocardial damage.

In the study of fatty acid metabolism, a variety of radionuclide tracers have been focused on evaluating fatty acid metabolism *in vivo* by using positron tracers. Among them, C-11 palmitate has long been used to probe fatty acid metabolism by PET.[68–72] However, there have been only a few reports with this technique partly due to the limited availability of PET and the complicated kinetic model. On the other hand, a variety of I-123 labeled fatty acid compounds have been introduced to probe myocardial energy metabolism *in vivo* in the routine clinical nuclear medicine facilities. Among them, I-123 labeled 15-(p-iodophenyl)-3R,S-methyl pentadecanoic acid (BMIPP) has been most extensively applied in clinical studies, particularly in Japan.

BMIPP is a branched fatty acids which goes into the myocardium and is long retaind in the cells with metabolic trapping, since methyl branching of the fatty acid chain may protect against metabolism via beta-oxidation.[73–75] Therefore, excellent myocardial image can be obtained with long residence time, which permits SPECT acquisition with the conventional rotatable camera.

Experimental studies slow clearance of approximately 25% of BMIPP in 2 hours.[76] The fractional distribution of these compounds at 30 minutes after tracer injection in rats indicated that 65 to 80% of the total activity resided in the triglyceride pool.[76] Our experimental studies indicated that BMIPP uptake correlated with the ATP concentration in acutely damaged myocardium treated with occlusion-reperfusion model[77] or dinitrophenol, an electron transport uncoupler.[78] In addition, the occlusion-reperfusion canine models showed abnormal BMIPP

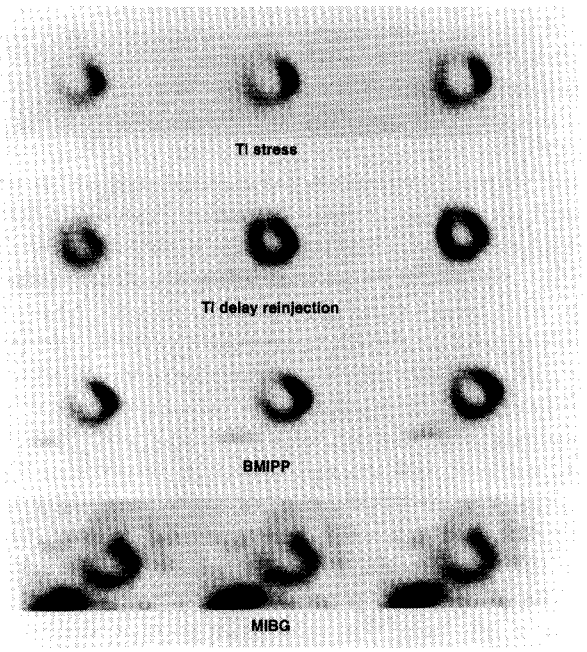

Fig. 4 A series of short-axis slices of stress and reinjection thallium images (top two rows), BMIPP images at rest (third row) and MIBG images at rest (bottom) of a patient with unstable angina. The thallium scan shows stress-induced ischemia in anteroseptal region. Similar abnormalities are identified in the same areas by both BMIPP and MIBG at rest, indicating metabolic alteration and neuronal dysfunction due to severe ischemia.

uptake which was different from thallium perfusion findings.[77,79,80] In comparison with PET findings, the BMIPP uptake correlated with the initial uptake of C-11 palmitate rather than the turnover rate of C-11 palmitate, indicating that BMIPP uptake may represent fatty acid uptake rather than β-oxidation of fatty acid.[81,82] Furthermore, the difference between BMIPP and thallium distribution which is often seen in the study of coronary artery disease may indicate ischemic myocardium where a perfusion-metabolism mismatch is seen on FDG-PET.[82,83] The discordant BMIPP uptake less than thallium may indicate suppression of fatty acid metabolism with metabolic shift from fatty acid to glucose utilization. In this sense, the combined BMIPP and thallium imaging may provide similar and important information as FDG-PET regarding the assessment of tissue viability.

Since BMIPP became commercially available in Japan in 1993, over 40,000 cases have been studied with this agent over three years. Following the administration of BMIPP, rapid myocardial uptake with long retention was observed, and therefore, high myocardial uptake is observed with low background with low uptake in the liver and the lung at 20–60 minutes after the BMIPP injection. BMIPP uptake is generally similar to thallium perfusion, but BMIPP uptake less than thallium perfusion (so called discordant BMIPP uptake) is often observed in a variety of diseases.

In the study of myocardial infarction, less BMIPP uptake than thallium perfusion in the areas of myocardial infarction was often observed.[84] Such discordant BMIPP uptake was often seen in recent onset of infarction, the areas with recanalized arteries, and those with severe wall motion abnormalities in comparison with thallium perfusion abnormality, indicating mostly metabolically stunned myocardium. Recent preliminary results showed that such discordant BMIPP uptake was observed in the areas associated with redistribution on stress thallium scan, indicating that such discordant areas may represent ischemic but viable myocardium.[85–87] The areas with discordant BMIPP uptake which is often observed in acute myocardial infarction may likely to improve perfusion and function in the subacute stage of infarction.[88,89] Such improvement is also observed after PTCA.[90] Most of them are associated with partial improvement in BMIPP uptake (Fig. 4). The difference between the defect scores for BMIPP and thallium correlates well with improvement in wall motion on the follow-up study. Similar findings have been reported by European groups using BMIPP and Tc-99m sestamibi.[91–93] These data indicate that the discordant BMIPP uptake in the acute stage of myocardial infarction may represent stunned myocardium where perfusion is almost normalized after reperfusion therapy on admission but regional wall motion abnormalities persist in association with sustained metabolic abnormalities.[94]

This concept has been extended to the study of ischemic heart disease without prior myocardial infarction. Abnormal BMIPP uptake at rest is often observed in the ischemic regions (Fig. 4). Such BMIPP findings are seen in severe myocardial ischemia and associated with regional wall motion abnormalities.[95–98] In addition, exercise BMIPP study has also been attempted to detect stress-induced metabolic abnormality.[99] Resting perfusion is often reduced but some cases there is normal perfusion at rest. These data indicate that BMIPP can reflect repetitive and/or severe prior ischemia, and thus, this may represent "ischemic memory imaging." It is quite controversial whether the areas with such discordant BMIPP uptake represent hibernating myocardium, and it may improve regional dysfunction after revascularization. However, since stunned myocardium is often mixed with myocardial hibernation in the clinical setting, areas of discordant BMIPP uptake may be likely to improve regional function after revascularization therapy.

On the basis of the concept that areas with discordant BMIPP uptake reflect severe ischemic myocardium associated with thallium redistribution and increase in FDG uptake, we hypothesized that this finding may have prognostic significance. In the follow-up of patients with prior myocardial infarction, those with discordant BMIPP uptake may be more likely to have future cardiac events than those without such findings.[100] Although these data remain quite preliminary, perfusion-metabolism mismatch

identified with SPECT tracers may play an important role for assessing ischemic but viable myocardium and risk stratification with a similar concept to FDG-PET.

III. Evaluation of adrenergic neuron function

With advance in biochemical imaging *in vivo* by the radionuclide technique, the modulation of the functional and electrophysiological properties of the heart by the autonomic nervous system has become the focus of intense research. The pathophysiologic role of the autonomic nervous system in patients with congestive heart failure has recently been emphasized.[101] For instance, the presence of heterogeneous sympathetic innervation is considered to be associated with fatal arrhythmias.[102] Tracer approaches are considered uniquely suited for *in vivo* characterization of neuronal structures and function in the myocardium by radionuclide imaging.

The autonomic nervous system consists of two main parts: sympathetic and parasympathetic innervation. Their major transmitters are norepinephrine and acetylcholine, respectively, which define the stimulatory and inhibitory physiological effect of each system. Sympathetic nerve fibers are characterized by multiple nerve endings which are filled with vesicles containing norepinephrine. Sympathetic nerve fibers travel parallel to the vascular structures on the epicardial surface of the heart and penetrate in to underlying myocardium in a similar fashion to the coronary vessels. On the basis of the tissue norepinephrine concentration, mammalian heart is characterized by dense adrenergic innervation with a norepinephrine concentration gradient from the atria to the base of the heart and from the base to the apex of the left ventricle.[103,104] These autonomic nervous systems involve the synthesis and storage of neurotransmitters, their release, reuptake, metabolism, and interaction with presynaptic and postsynaptic receptor sites. Such a complicated system cannot be characterized by a single radiopharmaceutical.

There are a number of radiotracers probing each step of autonomic neuronal functions. Of particular, norepinephrine analog has been widely used for experimental and clinical studies. In the early 1980s, I-131 labeled metaiodobenzylguanidine (MIBG), one of norepinephrine analogs was developed by a group in University of Michigan for selective mapping of sympathetic nerve ending in the heart.[105,106] This compound is an analog of the antihypertensive drug guanethidine, which is taken up and stored by the neurons followed by release along with endogenous norepinephrine on nerve stimulation, but this has low affinity for postsynaptic adrenergic receptors. I-123 labeled MIBG has been used in many clinical studies instead of the I-131 labeled one and yielded high quality images of myocardial neuron function images.[107,108] In recent experieace in the human studies, the normal distribution of MIBG in the myocardium may not be quite homogeneous with a slight reduction in the inferior region.[109] This heterogeneity seems to be more enhanced with age.[110] The interpretation of the MIBG images should be cautious with this physiological heterogeneity of the tracer distribution in the myocardium.

Different patterns of abnormal MIBG distribution in the myocardium indicating abnormalities in the cardiac sympathetic activity have been demonstrated after myocardial infarction,[111-114] dilated[115-117] and hypertrophic [118,119] cardiomyopathy, diabetic cardiomyopathy[120] and patients with idiopathic long QT syndrome[121] or arrhythmogenic right ventricular cardiomyopathy.[122]

Following myocardial infarction, decreased MIBG relative to thallium perfusion is observed as a evidence of denervation to varying degrees.[112] The transmural lesions showed denervation primarily distal and adjacent to the site of infarction. Transmural infarction produces necrosis of nerves coursing in the epicardium leading to viable but denervated myocardium.[111] This partial denervation may produce imbalanced sympathetic innervation, which may predispose the heart to arrhythmia.[123] Interestingly, nontransmural infarction is associated with myocardial denervation as an area of reduced MIBG uptake both in experimental and clinical studies.[112,124] Nontransmural infarction largely involves the subendocardium with the preserved subepicardial layer where the sympathetic nerve trunks are located. However, neuronal damage is often associated with severe myocardial ischemia despite the absence of myocardial necrosis. In this areas MIBG defect is usually larger than the thallium perfusion defect. Such denervation but viable myocardium is often observed in nontransmural infarction and some transmural infarction which is often reduced in size on the follow-up study.[125]

Although the sympathetic nerves are considered to be rather resistant to the effects of anoxia, some studies show histochemical evidence of nerve damage with diffusion of catecholamines after 30 min to 4 hour of ischemia.[126,127] Our experimental study showed the reduction of MIBG in the repetitive occlusion and reperfusion model.[128] In this model, the reduction of MIBG is associated with reduction of wall motion in the stunned myocardium. These experimental results can expand the clinical application of the detection of severe myocardial ischemia by MIBG. Actually the reduction in MIBG uptake in the myocardium is well demonstrated in patients with vasospastic angina[129] and unstable angina[125,130] (Fig. 4).

MIBG imaging may play additional important roles besides the detection of myocardial infarction and ischemia in the study of patients with coronary artery disease. One is the identification of sympathetic denervation in patients with tachyarrhythmia with underlying coronary artery disease.[113] In addition, regional sympathetic denervation showing MIBG defect was also demonstrated in structurally normal hearts in patients with ventricular arrhythmia.[131] The other is evaluation of the severity of heart failure, as a consequence of severe coronary artery disease. It is well

known that adrenergic dysfunction plays a key role in heart failure, and plasma catecholamine levels, for example, have been recognized as valuable prognostic tools. In patients with congestive heart failure, decreased retention and increased washout of MIBG from the myocardium is noted.[132–134] This may be due to increased plasma catecholamine concentration. In addition, increased sympathetic function together with a decrease in the number of uptake sites may play a key role in heart failure. More importantly, reduced MIBG uptake is considered to be a single and independent prognostic parameter among a variety of clinical parameters in the study of congestive heart failure.[135] Besides, recent experimental study showed the improvement of MIBG uptake in the failing heart after administration of renin-angiotensin converting enzyme inhibitor.[136] These data indicate that adrenergic neuronal fucntion analysis with MIBG is of clincial importance in the evaluation of coronary artery disease and associated conditions.

CONCLUSION

New techniques in nuclear cardiology have provided better accuracy in the detection of coronary artery disease on the basis of regional perfusion and function, but more importantly, they will permit precise tissue characterization, including metabolic alteration and neuronal function. This important information will play a key role in estimating severity and prognosis, and in planning the best strategy for managing these patients. Nevertheless, we are now entering a new era in nuclear cardiology. More clinical experience with the new techniques is required to confirm these exciting results.

REFERENCES

1. Bailey IK, Griffith LSC, Rouleay J, Strauss HW, Pitt B. Thallium-201 myocardial perfusion imaging at rest and during exercise: comparative sensitivity to eletrocardiography in coronary artery disease. *Circulation* 55: 79–87, 1977.
2. Pohost GM, Zir LM, Moore RH, McKusick KA, Guiney TE, Beller GA. Differentiation of transiently ischemic from infarcted myocardium by serial imaging after single dose of thallium-201. *Circulation* 55: 294–302, 1977.
3. Van Train KF, Berman DS, Garcia EV, Berger HJ, Sands MJ, Friedman JD, et al. Quantitative analysis of stress thallium-201 myocardial scintigrams: a multicenter trials. *J Nucl Med* 27: 17–25, 1986.
4. Jones AG, Abrams MJ, Davidson A, Brodack JW, Toothaker AK. Biological studies of a new class of technetium complexes: the hexakis (alkylisonitrile) technetium (I) cations. *Int J Nucl Med Biol* 11: 225–234, 1984.
5. Holman BL, Jones AG, Lister-James J, Davidson A, Abrams MJ, Kirshenbaum JM, et al. A new Tc-99m labeled myocardial imaging agent, hexakis (t-butylisonitrile)-technetium (I) (Tc-99m TBI): initial experience in the human. *J Nucl Med* 25: 1350–1355, 1984.
6. Taillefer R, Laflamme L, Dupras G, Picard M, Phaneuf DC, Leveille J. Myocardial perfusion imaging with ^{99m}Tc-methoxy-isobutyl-isonitrile (MIBI): comparison of short and long time intervals between rest and stress injections. *Eur J Nucl Med* 13: 515–522, 1988.
7. Kahn JK, MciGhie I, Akers MS, Sills MN, Faber TL, Kulkarni PV, et al. Quantitative rotational tomography with ^{201}Tl and ^{99m}Tc 2-methoxy-isobutyl-isonitrile: a direct comparison in normal individuals and patients with coronary artery disease. *Circulation* 79: 1282–1293, 1989.
8. Wackers FJT, Berman DS, Maddahi J, Watson DD, Beller GA, Strauss HW, et al. Technetium-99m hexakis 2-methoxyisobutyl isonitrile: human biodistribution, dosimetry, safety, and preliminary comparison to thallium-201 for myocardial perfusion imaging. *J Nucl Med* 30: 301–311 1989.
9. Maisey MN, Lowry A, Bischof-Delaloye AB, Fridrich R, Inglese E, Khalil MN, et al. European multi-centre comparison of thallium-201 and technetium-99m methoxyisobutyl-isonitrile in ischemic heart disease. *Eur J Nucl Med* 16: 869–872, 1990.
10. Lahiri A, Higley B, Kelly JD, et al. Myocardial perfusion imaging in man using new ^{99m}Tc functionalised disphophine complexes. *Eur J Nucl Med* 15: 425, 1989.
11. Higley B, Smith FW, Smith T, Gemmell HG, DasGupta P, Gvozdanovic DV, et al. Technetium-99m-1,2-bis (bis(2-ethoxyethyl)phosphino)ethane: human biodistribution dosimetry and safety of a new myocardial perfusion imaging agent. *J Nucl Med* 34: 30–38, 1993.
12. Tamaki N, Takahashi N, Kawamoto M, et al. Myocardial tomography using technetium-99m-tetrofosmin to evaluate coronary artery disease. *J Nucl Med* 35: 594–600, 1994.
13. Rigo P, Leclercq B, Itti R, et al. Technetium-99m-tetrofosmin myocardial imaging: a comparison with thallium-201 and angiography. *J Nucl Med* 35: 587–593, 1994.
14. Matsunari I, Fujino S, Taki J, et al. Comparison of defect size between thallium-201 and technetium-99m tetrofosmin myocardial single-photon emission computed tomography in patients with single-vessel coronary artery disease. *Am J Cardiol* 77: 350–354, 1996.
15. Sporn V, Balino NP, Holman BL, Liprandi AS, Masoli O, Mitta A, et al. Simultaneous measurement of ventricular function and myocardial perfusion using the technetium-99m isonitriles. *Clin Nucl Med* 13: 77–81, 1988.
16. Baillet GY, Mena IG, Kuperus JH, Robertson JM, French WJ. Simultaneous technetium-99m MIBI angiography and myocardial perfusion imaging. *J Nucl Med* 30: 38–44, 1989.
17. Iskandrian AS, Heo J, Kong B, Lyons E, Marsch S. Use of technetium-99m isonitrile (RP-30A) in assessing left ventricular perfusion and function at rest and during exercise in coronary artery disease, and comparison with coronary arteriography and exercise thallium-201 SPECT imaging. *Am J Cardiol* 64: 270–275, 1989.
18. Borges-Neto S, Coleman RE, Jones RH. Perfusion and function at rest and treadmill exercise using technetium-99m-sestamibi: comparison of one- and two-day protocols in normal volunteers. *J Nucl Med* 31: 1128–1132, 1990.
19. Villaneva-Meyer J, Mena I, Narahara KA. Simultaneous assessment of left ventricular wall motion and myocardial

perfusion with technetium-99m-methoxy isobutyl isonitrile at stress and rest in patients with angina; comparison with thallium-201 SPECT. *J Nucl Med* 31: 457–463, 1990.
20. Takahashi N, Tamaki N, Tadamura E, et al. Combined assessment of regional perfusion and wall motion in patients with coronary artery disease with technetium-99m tetrofosmin. *J Nucl Cardiol* 1: 29–38, 1994.
21. Manning F, Morgan-Manning MG. Gated SPECT with technetium-99m-sestamibi for assessment of myocardial perfusion abnormalities. *J Nucl Med* 34: 601–608, 1993.
22. Cook CD, Garcia EV, Cullom SJ, et al. Determinating the accuracy of calculation systolic wall thickening using a Fourier transform approximation: a simulation study based on canine and patient data. *J Nucl Med* 35: 1185–1192, 1994.
23. Williams KA, Taillon LA. Left ventricular function in patients with coronary artery disease assessed by gated tomographic myocardial perfusion images. *J Am Coll Cardiol* 27: 173–181, 1996.
24. Anagnostopoulos C, Gunning MG, Pannell DJ, et al. Regional myocardial motion and thickening assessed at rest by ECG-gated ^{99m}Tc-MIBI emission tomography and by magnetic resonance imaging. *Eur J Nucl Med* 23: 909–916, 1996.
25. Pierard LC, DeLandsheere CM, Berthe C, et al. Identification of viable myocardium by echocardiography during dobutamine infusion in patients with myocardial infarction after thrombolytic therapy: comparison with positron emission tomography. *J Am Coll Cardiol* 15: 1021–1031, 1990.
26. Cohn JN, Rector TS. Prognosis of congestive heart failure and predictors of mortality. *Am J Cardiol* 62: 25A–30A, 1988.
27. Lee KL, Pryor DB, Pieper KS, et al. Prognostic value of radionuclide angiography in medically treated patients with coronary artery disease: a comparison with clinical and catheterization variables. *Circulation* 82: 1705–1717, 1990.
28. Iskandrian AS, Hakki AH, Kane-Marsch S. Prognostic implications of exercise thallium-201 scintigraphy in patients with suspected or known coronary artery disease. *Am Heart J* 110: 135–143, 1985.
29. Kaul S, Lilly DR, Gascho GA, et al. Prognostic utility of the exercise thallium-201 test in ambulatory patients with chest pain: comparison with cardiac catheterization. *Circulation* 77: 745–758, 1988.
30. Palmas W, Friedman JD, Diamond GA, et al. Incremental value of simultaneous assessment of myocardial function and perfusion with technetium-99m sestamibi for prediction of extent of coronary artery disease. *J Am Coll Cardiol* 25: 1024–1031, 1995.
31. Nallamouthu N, Araujo L, Russell J, et al. Prognostic value of simultaneous perfusion and function assessment using Technetium-99m sestamibi. *Am J Cardiol* 76: 562–564, 1996.
32. Braunwald E, Kloner RA. The stunned myocardium: prolonged, postischemic ventricular dysfunction. *Circulation* 66: 1146–1149, 1982.
33. Gibbons RJ, Verani MS, Behrenbeck T, et al. Feasibility of tomographic technetium-99m-hexakis-2-methoxy-2-methylisopropyl-isonitrile imaging for the assessment of myocardial area at risk and the effect of acute treatment in myocardial infarction. *Circulation* 80: 1277–1286, 1989.
34. Wackers FJ, Verani MS, Behrenbeck T, et al. Serial quantitative planar technetium-99m-isonitrile imaging in acute myocardial infarction: efficacy for noninvasive assessment of thrombolytic therapy. *J Am Coll Cardiol* 14: 861–873, 1989.
35. Sinusas AJ, Trautman KA, Bergin JD, et al. Qunatification of area at risk during coronary occlusion and degree of myocardial salvage after reperfusion with technetium-99m-methoxy isobutyl isonitrile. *Circulation* 82: 1424–1437, 1990.
36. Rocco TP, Dilsizian V, Strauss HW, et al. Technetium-99m isonitrile myocardial uptake at rest. II. Relation to clincial markers of potential viability. *J Am Coll Cardiol* 14: 1678–1684, 1989.
37. Medrano R, Lowry RW, Young JB, et al. Assessment of myocardial viability with ^{99m}Tc-sestamibi in patient undergoing cardiac transplantation. *Circulation* 94: 1010–1017, 1996.
38. Takahashi N, Reinhardt CP, Marcel R, Leppo JA. Myocardial uptake of ^{99m}Tc-tetrofosmin, sestamibi and ^{201}Tl in a model of acute coronary reperfusion. *Circulation* 94: 2605–2613, 1996.
39. Udelson JE, Coleman PS, Metherall J, et al. Predicting recovery of severe regional ventricular dysfunction: comparison of resting scintigraphy with ^{201}Tl and ^{99m}Tc-sestamibi. *Circulation* 89: 2552–2561, 1994.
40. Altefoefer C, Kaiser HJ, Dorr R, et al. Fluorine-18 deoxyglucose PET for assessment of viable myocardium in perfusion defects in ^{99m}Tc-MIBI SPET: a comparative study in patients with coronary artery disease. *Eur J Nucl Med* 19: 334–342, 1992.
41. Sawada SG, Allman KC, Muzik O, et al. Positron emission tomography detects evidence of viability in rest technetium-99m sestamibi defects. *J Am Coll Cardiol* 23: 92–98, 1994.
42. Dilsizian V, Arrighi JA, Diodati JG, et al. Myocardial viability in patients with chronic coronary artery disease: comparison of ^{99m}Tc-sestamibi with thallium reinjection and ^{18}F-fluorodeoxyglucose. *Circulation* 89: 578–587, 1994.
43. Phelps M, Hoffman E, Selin C, et al. Investigation of ^{18}F-2-fluoro-2-deoxyglucose for the measure of myocardial glucose metabolism. *J Nucl Med* 19: 1311–1319, 1978.
44. Neely JR, Rovetto M, Oram J. Myocardial utilization of carbohydrate and lipids. *Prog Cardiovasc Dis* 15: 289–329, 1972.
45. Liedke AJ. Alterations of carbohydrate and lipid metabolism in the acutely ischemic heart. *Prog Cardiovasc Dis* 23: 321–336, 1981.
46. Camici P, Ferrannini E, Opie L. Myocardial metabliosm in ischemic heart disease; basic principles and application to imaging by positron emission tomography. *Prog Cardiovasc Dis* 32: 217–238, 1989.
47. Marshall RC, Tillisch JH, Phelps ME, et al. Identification and differentiation of resting myocardial ischemia and infarction in man with positron computed tomography, ^{18}F-labeled fluorodeoxyglucose and N-13 ammonia. *Circulation* 67: 766–778, 1983.
48. Tillisch J, Brunken R, Marshall R, Schwaiger M, Mandelkern M, Phelps M, et al. Reversibility of cardiac wall-motion abnormalities predicted by positron tomography. *N Eng J Med* 314: 884–888, 1986.

49. Tamaki N, Yonekura Y, Yamashita K, Saji H, Magata Y, Senda M, et al. Positron emission tomography using fluorine-18 deoxyglucose in evaluation of coronary artery bypass grafting. *Am J Cardiol* 64: 860–865, 1989.
50. Marwick T, MacIntyre W, LaFont A, et al. Metabolic responses of hibernating and infarcted myocardium to revascularization: a follow-up study of regional perfusion, function, and metabolism. *Circulation* 85: 1347–1353, 1992.
51. Lucignani G, Paolioni G, Landoni C, et al. Presurgical identification of hibernating myocardium by combined use of technetium-99m hexakis 2-methylisobutylisonitrile single photon emission tomography and fluorine-18 fluoro-2-deoxy-D-glucose positron emission tomography in patients with coronary artery disease. *Eur J Nucl Med* 19: 874–881, 1992.
52. Tamaki N, Kawamoto M, Tadamura E, et al. Prediction of reversible ischemia after revascularization: perfusion and metabolic studies with positron emission tomography. *Circulation* 91: 1697–1705, 1995.
53. Brunken R, Tillisch J, Schwaiger M, et al. Regional perfusion, glucose metabolism, and wall motion in patients with chronic electrocardiographic Q wave infarctions: evidence for persistence of viable tissue in some infarct regions by positron emission tomography. *Circulation* 73: 951–963, 1986.
54. Tamaki N, Yonekura Y, Yamashita K, Senda M, Saji H, Hashimoto T, et al. Relation of left ventricular perfusion and wall motion with metabolic activity in persistent defects on thallium-201 tomography in healed myocardial infarction. *Am J Cardiol* 62: 202–208, 1988.
55. Brunken R, Schwaiger M, Grover-McKay M, Phelps ME, Tillisch J, Schelbert HR. Positron emission tomography detects tissue metabolic activity in myocardial segments with persistent thallium perfusion defects. *JACC* 10: 557–567, 1987.
56. Brunken R, Kottou S, Nienaber CA, Schwaiger M, Ratib OM, Phelps ME, et al. PET detection of viable tissue in myocardial segments with persistent defect at Tl-201 SPECT. *Radiology* 65: 65–73, 1989.
57. Bonow RO, Dilsizian V, Cuocolo A, Bacharach SL. Identification of viable myocardium in patients with coronary artery disease and left ventricular dysfunction: comparison of thallium scintigraphy with reinjection and PET imaging with ^{18}F-fluorodeoxyglucose. *Circulation* 83: 26–37, 1991.
58. Tamaki N, Ohtani H, Yamashita K, Magata Y, Yonekura Y, Nohara R, et al. Metabolic activity in the areas of new-fill-in after thallium-201 reinjection: comparison with positron emission tomography using fluorine-18-deoxyglucose. *J Nucl Med* 32: 673–678, 1991.
59. Eitzman D, Al-Aouar Z, Kanter HL, von Dahl J, Kirsh M, Deeb GM, et al. Clinical outcome in patients with advanced coronary artery disease after viability studies with positron emission tomography. *J Am Coll Cardiol* 20: 559–565, 1992.
60. Tamaki N, Kawamoto M, Takahashi N, et al. Prognostic value of an increase in fluorine-18 deoxyglucose uptake in patients with myocardial infarction: comparison with stress thallium imaging. *J Am Coll Cardiol* 22: 1621–1627, 1993.
61. Di Carli M, Davidson M, Little R, et al. Value of metabolic imaging with positron emission tomography for evaluating prognosis in patients with coronary artery disease and ventricular dysfunction. *Am J Cardiol* 73: 527–533, 1994.
62. Brown M, Marshall DR, Sobel BE, Bergmann SR. Delineation of myocardial utilization with carbon-11-labeled acetate. *Circulation* 76: 687–696, 1987.
63. Buxton DB, Schwaiger M, Nguyen A, Phelps ME, Schelbert MR. Radiolabeled acetate as a tracer of myocardial tricarboxylic acid cycle flux. *Cir Res* 63: 628–634, 1988.
64. Tamaki N, Magata Y, Takahashi N, Kawamoto M, Torizuka T, Yonekura Y, et al. Myocardial oxidative metabolism in normal subjects in fasting, glucose loading and dobutamine infusion states. *Ann Nucl Med* 6: 221–228, 1992.
65. Gropler RJ, Geltman EM, Sampathkumaran K, Perez JE, Moerlein SM, Sobel BE, et al. Functional recovery after coronary revascularization for chronic coronary artery disease is dependent on maintenance of oxidative metabolism. *J Am Coll Cardiol* 20: 69–77, 1992.
66. Weinheimer CJ, Brown MA, Nohara R, Perez JE, Bergmann SR. Functional recovery after reperfusion is predicated on recovery myocardial oxidative metabolism. *Am Heart J* 125: 939–949, 1993.
67. Hata T, Nohara R, Tamaki N, et al. Noninvasive assessment of myocardial viability by positron emission tomography with ^{11}C-acetate in patients with old myocardial infarction. *Circulation* 94: 1834–1841, 1996.
68. Weiss ES, Hoffman EJ, Phelps ME, Welch MJ, Henry PD, Ter-Pogossian MM, et al. External detection and visualization of myocardial ischemia with C-11 substrates *in vivo* and *in vitro*. *Circ Res* 39: 24–32, 1976.
69. Sobel BE, Weiss ES, Welch MJ, Siegel BA, Ter-Pogosian MM. Detection of remote myocardial infarction in patients with positron transaxial tomography and intravenous C-11 palmitate. *Circulation* 55: 853–857, 1977.
70. Schon HR, Schelbert HR, Robinson G, Najafi A, Huang SC, Hansen H, et al. C-11 labeled palmitic acid for the noninvasive evaluation of regional myocardial fatty acid metabolism with positron computed tomography. I. Kinetics of C-11 palmitic acid in normal myocardium. *Am Heart J* 103: 532–547, 1982.
71. Schon HR, Schelbert HR, Nahaji A, Hansen H, Huang H, Barrio J, et al. C-11 labeled palmitic acid for the noninvasive evaluation of regional myocardial fatty acid metabolism with positron computed tomography. II. Kinetics of C-11 palmitic acid in acutely ischemic myocardium. *Am Heart J* 103: 548–561, 1982.
72. Tamaki N, Fujibayashi Y, Magata Y, et al. Radionuclide assessment of myocardial fatty acid metabolism by PET and SPECT. *J Nucl Cardiol* 2: 256–266, 1995.
73. Otto CA, Brown LE, Scott AM. Radioiodinated branch-chain fatty acids: substrates for beta oxidation? *J Nucl Med* 25: 75–80, 1984.
74. Knapp FF, Kropp J. Iodine-123-labeled fatty acids for myocardial single-photon emission tomography. *Eur J Nucl Med* 22: 361–381, 1995.
75. Knapp FF, Goodman MM, Kirsch G, et al. Both total chain length and position of dimethyl-branching effect the myocardial uptake and retention of radioiodinated analogues of 15-(p-iodophenyl)-3,3-dimethyl pentadecanoic acid (DMIPP). *Ann Nucl Med* 10: 19–32, 1996.
76. Ambrose KR, Owen BA, Goodman MM, Knapp FF Jr. Evaluation of the metabolism in rat heart of two new radioiodinated 3-methyl-branched fatty acid myocardial

imaging agents. *Eur J Nucl Med* 12: 486–491, 1987.
77. Nohara R, Okuda K, Ogino M, et al. Evaluation of myocardial viability with iodine-123-BMIPP in a canine model. *J Nucl Med* 37: 1403–1407, 1996.
78. Fujibayashi Y, Yonekura Y, Takemura Y, et al. Myocardial accumulation of iodinated beta-methyl-branched fatty acid analogue, iodine-125-15-(p-iodophenyl)-3-(R,S)methylpentadecanoic acid (BMIPP), in relation to ATP concentration. *J Nucl Med* 31: 1818–1822, 1990.
79. Miller DD, Gill JB, Elmaleh D, Aretz T, Boucher CA, Strauss HW. Fatty acid analogue accumulation: a marker of myocyte viability in ischemic-reperfused myocardium. *Circ Res* 63: 681–692, 1988.
80. Nishimura T, Sago M, Kihara K, et al. Fatty acid myocardial imaging using ^{123}I-β-methyl-iodophenyl pentadecanoic acid (BMIPP): comparison of myocardial perfusion and fatty acid utilization in canine myocardial infarction (occlusion and reperfusion model). *Eur J Nucl Med* 15: 341–345, 1989.
81. Kawamoto M, Tamaki N, Yonekura Y, Magata Y, Tadamura E, Nohara R, et al. Significance of myocardial uptake of I-123 beta-methyl iodophenyl pentadecanoic acid: comparison with kinetics of C-11 palmitate. *J Nucl Cardiol* 1: 522–528, 1994.
82. Tamaki N, Kawamoto M. The use of iodinated free fatty acids for assessing fatty acid metabolism. *J Nucl Cardiol* 1: S72–78, 1994.
83. Tamaki N, Tadamura E, Kawamoto M, et al. Decreased uptake of iodinated branched fatty acid analogue indicates metabolic alterations in ischemic myocardium. *J Nucl Med* 36: 1974–1980, 1995.
84. Tamaki N, Kawamoto M, Yonekura Y, Fujibayashi Y, Takahashi N, Konishi J, et al. Regional metabolic abnormality in relation to perfusion and wall motion in patients with myocardial infarction: assessment with emission tomography using an iodinated branched fatty acid. *J Nucl Med* 33: 659–667, 1992.
85. Kawamoto M, Tamaki N, Yonekura Y, Tadamura E, Fujibayashi Y, Magata Y, et al. Combined study with I-123 fatty acid and thallium-201 to assess ischemic myocardium. *Ann Nucl Med* 8: 47–54, 1994.
86. Matsunari I, Saga T, Taki J, et al. Kinetics of iodine-123-BMIPP in patients with prior myocardial infarction: assessment with dynamic rest and stress images compared with stress thallium-201 SPECT. *J Nucl Med* 35: 1279–1285, 1994.
87. Tawarahara K, Kurata C, Taguchi T, et al. Simultaneous dual myocardial imaging with iodine-123-β-methyl iodophenyl-pentadecanoic acid (BMIPP) and thallium-201 in patients with coronary artery disease. *Jpn Circ J* 58: 107–115, 1994.
88. Ito T, Tanouchi J, Kato J, et al. Recovery of impaired left ventricular function in patients with acute myocardial infarction is predicted by the discordance on defect size on ^{123}I-BMIPP and ^{201}Tl-SPET images. *Eur J Nucl Med* 23: 917–923, 1996.
89. Hashimoto A, Nakata T, Tsuchihashi K, et al. Postischemic functional recovery and BMIPP uptake after pulmonary percutaneous transluminal coronary angioplasty in acute myocardial infarction. *Am J Cardiol* 77: 25–30, 1996.
90. Matsunari I, Saga T, Taki J, et al. Improved myocardial fatty acid utilization after percutaneous transluminal coronary angioplasty. *J Nucl Med* 36: 1605–1607, 1995.
91. De Geeter F, Franken PR, Bossuyt A. Relationship between blood flow and fatty acid metabolism in subacute myocardial infarction: a study means of ^{99m}Tc-sestamibi and ^{123}I-β-methyl-iodophenyl pentadecanoic acid. *Eur J Nucl Med* 21: 283–291, 1994.
92. Franken PR, De Geeter F, Dendale P, et al. Abnormal free fatty acid uptake in subacute myocardial infarction after coronary thrombolysis: correlation with wall motion and inotropic reserve. *J Nucl Med* 35: 1758–1765, 1994.
93. Franken PR, Dendale P, De Geeter F, et al. Prediction of functional outcome after myocardial infraction using BMIPP and sestamibi scintigraphy. *J Nucl Med* 37: 718–722, 1996.
94. Schwaiger M, Schelbert HR, Ellison D, et al. Sustained regional abnormalities in cardiac metabolism after transient ischemic in the chronic dog model. *J Am Coll Cardiol* 6: 336–347, 1985.
95. Matsunari I, Saga T, Taki J, et al. Relationship between various parameters derived from ^{123}I-lalebed beta-methyl-branched fatty acid whole-body scintigraphy and left ventricular ejection fraction in patients with ischaemic heart disease. *Nucl Med Commun* 15: 685–689, 1994.
96. Takeishi Y, Atsumi H, Fujiwara S, et al. Fatty acid metabolic imaging with ^{123}I-BMIPP for the diagnosis of coronary artery disease. *Nucl Med Commun* 17: 675–680, 1996.
97. Taki J, Nakajima K, Matsunari I, et al. Impairment of regional fatty acid uptake in relation to wall motion and thallium-201 uptake in ischaemic but viable myocardium. *Eur J Nucl Med* 22: 1385–1392, 1995.
98. Fukuzawa S, Inagaki M, Morooka S, et al. An effective tool to detect lesions causing unstable angina with multivessel disease. *J Cardiol* 28: 191–198, 1996.
99. Mori T, Hayakawa M, Hattori K, et al. Exercise β-methyl iodophenyl pentadecanoic acid (BMIPP) and resting thallium delayed single-photon emission computed tomography (SPECT) in the assessment of ischemia and viability. *Jpn Circ J* 60: 17–26, 1996.
100. Tamaki N, Tadamura E, Kudoh T, et al. Prognostic value of iodine-123 labelled BMIPP fatty acid analogues imaging in patients with myocardial infarction. *Eur J Nucl Med* 23: 272–279, 1996.
101. Bristow M, et al. Decreased catecholamine sensitivity and beta-adrenergic-receptor density in failing heart. *N Engl J Med* 307: 205–207, 1982.
102. Inoue H, Zipes DP. Results of sympathetic denervation in the canine heart: supersensitivity that may be arrhythmogenic. *Circulation* 75: 877–887, 1987.
103. Shore PA, Cohn VH, Highman B, Maling H. Distribution of norepinephrine in the heart. *Nature* 181: 848–849, 1958.
104. Randall W, Armour JA, Geis P, Lippencott D. Regional cardiac distribution of sympathetic nerves. *Federation Proc* 31: 199–208, 1972.
105. Wieland DM, Wu J-I, Brown LE, et al. Radiolabeled adrenergic neuron-blocking agents: adrenomedullary imaging with (I-131) iodobenzyl-guanidine. *J Nucl Med* 21: 349–353, 1980.
106. Nakajo M, Shapiro B, Copp J, et al. The normal and abnormal distribution of the adrenomedullary imaging agent m-[I-131]iodobenzylguanidine (I-131 MIBG) in man: evaluation by scintigraphy. *J Nucl Med* 24: 672–682, 1983.

107. Kline RC, Swanson DP, Wieland DM, et al. Myocardial imaging in man with I-123 metaiodobenzylguanidine. *J Nucl Med* 22: 129–132, 1981.
108. Sisson JC, Shapiro B, Meyers L, et al. Meta-iodobenzylguanidine to map scintigraphically the adrenergic nervous system in man. *J Nucl Med* 28: 1625–1636, 1987.
109. Gill JS, Hunter GJ, Gane G, Camm AJ. Heterogeneity of the human myocardial sympathetic innervation: *in vivo* demonstration by iodine-123-labeled metaiodobenzylguanidine scintigraphy. *Am Heart J* 126: 390–398, 1993.
110. Tsuchimochi S, Tamaki N, Tadamura E, et al. Age and gender differences in normal myocardial adrenergic neuronal function evaluated by iodine-123-MIBG imaging. *J Nucl Med* 36: 969–974, 1995.
111. Barber MJ, Mueller TM, Henry DP, et al. Transmural myocardial infarction in the dog produces sympathectomy in noninfarcted myocardium. *Circulation* 67: 787–796, 1983.
112. Dae MW, Herre JM, O'Connell JW, et al. Scintigraphic assessment of sympathetic innervation after transmural versus nontransmural myocardial infarction. *J Am Coll Cardiol* 17: 1416–1423, 1991.
113. Stanton MS, Mahmoud MM, Radtke NL, et al. Regional sympathetic denervation after myocardial infarction in humans detected noninvasively using I-123-metaiodobenzylguanidine. *J Am Coll Cardiol* 14: 1519–1526, 1989.
114. McGhie AI, Corbett JR, Akers MS, et al. Regional cardiac adrenergic function using I-123-meta-iodobenzylguanidine tomographic imaging after acute myocardial infarction. *Am J Cardiol* 67: 236–242, 1991.
115. Glowniak JV, Turner FE, Gray LL, et al. Iodine-123 metaiodobenzylguanidine imaging of the heart with idiopathic congestive cardiomyopathy and cardiac transplants. *J Nucl Med* 30: 1182–1191, 1989.
116. Schofer J, Spielmann R, Schuchert A, et al. Iodine-123 metaiodobenzylguanidine scintigraphy: a noninvasive method to demonstrate myocardial adrenergic nervous system disintegrity in patients with idiopathic dilated cardiomyopathy. *J Am Coll Cardiol* 12: 1252–1258, 1988.
117. Henderson EB, Kahn JK, Corbett JR, et al. Abnormal I-123 metaiodobenzylguanidine myocardial washout and distribution may reflect myocardial adrenergic derangement in patients with congestive cardiomyopathy. *Circulation* 78: 1192–1199, 1988.
118. Nakajima K, Bunko H, Taki J, et al. Quantitative analysis of ^{123}I-meta-iodobenzylguanidine (MIBG) uptake in hypertrophic cardiomyopathy. *Am Heart J* 119: 1329–1337, 1990.
119. Taki J, Nakajima K, Bunko H, et al. Whole-body distribution of iodine 123-metaiodobenzylguanidine in hypertrophic cardiomyopathy: significance of its washout from the heart. *Eur J Nucl Med* 17: 264–268, 1990.
120. Hattori N, Tamaki N, Hayashi T, et al. I-123-Metaiodobenzylguanidine (MIBG) to assess cardiac denervation in diabetic patients: value of regional distribution index. *J Nucl Med* 37: 1985–1990, 1996.
121. Gohl K, Feistel H, Weikl A, et al. Congenital myocardial sympathetic dysinnervation (CMSD)—a structural defect of idiopathic long QT syndrome. *PACE* 14: 1544–1553, 1991.
122. Wichter T, Hindricks G, Lerch H, et al. Regional myocardial sympathetic dysinnervation in arrhythmogenic right ventricular cardiomyopathy. *Circulation* 89: 667–683, 1994.
123. Herre JM, Westein L, Lin YL, et al. Effect of transmural versus nontransmural myocardial infarction on inducibility of ventricular arrhythmias during sympathetic stimulation in dogs. *J Am Coll Cardiol* 2: 413–421, 1988.
124. Tomoda H, Yoshioka K, Shiina Y, et al. Regional sympathetic denervation detected by iodine 123 metaiodobenzylguanidine in non-Q-wave myocardial infarction and unstable angina. *Am Heart J* 128: 452–458, 1994.
125. Nishimura T, Oka H, Sago M, et al. Serial assessment of denervated but viable myocardium following acute myocardial infarction in dogs using iodine-123 metaiodobenzylguanidine and thallium-201 chloride myocardial single photon emission tomography. *Eur J Nucl Med* 19: 25–29, 1992.
126. Holmgren S, Abrahamson T, Almgren O. Adrenergic innervation of coronary arteries and ventricular myocardium in the pig: fluorescence microscopic appearance in the normal state and after ischemia. *Basic Res Cardiol* 80: 18–26, 1985.
127. Mathes P, Cowan C, Gudbjanason S. Storage and metabolism of norepinephrine after experimental myocardial infarction. *Am J Physiol* 220: 27–32, 1971.
128. Nohara R, Kambara H, Tamaki N, et al. Effect of cardiac sympathetic nervous system on the stunned myocardium: experimental study with ^{123}I-metaiodobenzylguanidine. *Jpn Circulation J* 55: 893–899, 1991.
129. Takano H, Nakamura T, Satou T, et al. Regional myocardial sympathetic dysinnervation in patients with coronary vasospasm. *Am J Cardiol* 75: 324–239, 1995.
130. Tsutsui H, Ando S, Fukai T, et al. Detection of angina-provoking coronary stenosis by resting iodine-123 metaiodobenzylguanidine scintigraphy in patients with unstable angina. *Am Heart J* 129: 708–715, 1995.
131. Mitrani RD, Klein LS, Miles WM, et al. Regional cardiac sympathetic denervation in patients with ventricular tachycardia in the absence of coronary artery disease. *J Am Coll Cardiol* 22: 1344–1353, 1993.
132. Rabinovitch MA, Rose CP, Rouleau JL, et al. Metaiodobenzylguanidine [^{123}I] scintigraphy detects impaired myocardial sympathetic neuronal transport function of canine mechanical-overload heart failure. *Cir Res* 61: 797–804, 1987.
133. Rabinovitch MA, Rose CP, Schwab AJ, et al. A method of dynamic analysis of iodine-123-metaiodobenzylguanidine scintigrams in cardiac mechanical overload hypertrophy and failure. *J Nucl Med* 34: 589–600, 1993.
134. Bohm M, LaRosee K, Schwinger RHG, et al. Evidence for reduction of norepinephrine uptake sites in the failing human heart. *J Am Coll Cardiol* 25: 146–153, 1995.
135. Merlet P, Valette H, Dubois-Rande J-L, et al. Prognostic value of cardiac metaiodobenzylguanidine imaging in patients with heart failure. *J Nucl Med* 33: 471–477, 1992.
136. Takatsu H, Uno Y, Fujiwara H. Modulation of left ventricular iodine-125-MIBG accumulation in cardiomyopathic Syrian hamster using the renin-angiotensin system. *J Nucl Med* 36: 1055–1061, 1995.